Thermochromism and Dynamics of Organometallic Conjugated Systems: Zirconocene Complex of 1,4-Diphenyl-1,3-butadiene

Sadamu Takeda,*,† Hiroki Fukumoto,‡ Kazushi Mashima,§ Goro Maruta,† Kizashi Yamaguchi,† and Akira Nakamura‡

Department of Chemistry and Department of Macromolecular Science, Faculty of Science, Osaka University, Toyonaka, Osaka 560, Japan, and Department of Chemistry, Faculty of Engineering Science, Osaka University, Toyonaka, Osaka 560, Japan

Received: July 3, 1996; In Final Form: September 26, 1996[⊗]

We observed the thermochromism of the deeply colored zirconocene complex of 1,4-diphenyl-1,3-butadiene (DPBD) in the solid state. Variable-temperature ^{13}C-CP/MAS NMR spectroscopy revealed that a remarkable change of the electronic structure of the DPBD molecule by constructing the complex propagates all over the carbon sites and that the distortion of the electronic structure of the complex becomes continuously large as temperature is decreased. This phenomenon is closely related to the thermochromism. The mechanism of the temperature variation of the electronic structure of the complex was attributed to the dynamics of phenyl ring and cyclopentadienyl ring of the complex. Fast rotation of the cyclopentadienyl ring around its fivefold axis with the extremely small activation energy of 28 meV (=2.6 kJ/mol) and 180° flip rotation of the phenyl ring about the C−C bond with the activation energy of 84 meV (=7.7 kJ/mol) were recognized by the measurement of the spin−lattice relaxation rate of proton NMR. Semiempirical ZINDO molecular orbital calculation revealed that the deep color of the complex originates in the HOMO−LUMO and HOMO−LUMO+1 transitions. These molecular orbitals are sensitive to the orientation of the π-orbital of cyclopentadienyl rings, suggesting that the dynamic perturbation is operative for the transition energies.

Introduction

Conjugation in organic compounds is represented by extended pπ−pπ interactions. *trans*-Polyacetylene is a typical and fascinating one-dimensional conjugated system. Many interesting physical and chemical properties have been found for this pπ conjugated system upon doping.[1] A modified conjugation and/or doping category can be seen in organometallic systems, in which extended π-interaction involving metal−carbon bonding is realized.[2] The uniqueness of the organometallic π-systems containing various transition metals exists because of their large variety of the electronic and molecular structures. An example is metal π-complexes of organic conjugated systems. Particularly, polyene complexes of early transition metals such as zirconium are interesting, since these electron-deficient metal ions are highly reactive and thus the polyene system may be largely perturbed by the bonding with zirconium which is both electron donating (π-type) and attracting (σ-type) in varying degrees. The situation is basically different from the simple doping of conventional conjugated systems.

The simplest polyene is diene and the diene complexes of transition metals are known to prefer mostly the *s-cis* conformation.[3] The complexes of *s-trans* coordination have recently prepared for the early transition metals, *e.g.* $ZrCp_2$(DPBD) (Cp = C_5H_5, DPBD = 1,4-diphenyl-1,3-butadiene),[3−7] Mo(NO)-Cp(1,3-butadiene),[8] $NbCp(C_4H_6)_2$.[9] For the *s-trans* coordinated complex, π-conjugation of the diene molecule is maintained and the effect of mixing of the d-electron of the transition metal may be delocalized over the diene molecule. Thus a mixed electronic state of organic pπ-electron and metallic d-electron is expected for this type of compound.

$ZrCp_2$(DPBD) consists of zirconocene ($ZrCp_2$) and 1,4-diphenyl-1,3-butadiene molecule which has large π-conjugated system among the *s-trans* coordinated 1,3-diene complexes mentioned above. The color of the polycrystals of this complex is in between deep red and deep purple, while the precursors of the complex, $ZrCp_2Cl_2$ and 1,4-diphenyl-1,3-butadiene, are almost colorless. The deep color is a character of the hybridized electronic state of the organic π- and metallic d-systems. We observed a remarkable thermochromism for this compound in the solid state. The color of the polycrystals changes continuously as the temperature is decreased from room temperature to liquid nitrogen temperature. This phenomenon suggests that the hybridized electronic state of the complex $ZrCp_2$(DPBD) is coupled to a thermal perturbation.

In this paper, we report the variable-temperature ^{13}C-CP/MAS NMR measurements to characterize the interaction between the zirconocene and DPBP molecule and to reveal the temperature variation of the electronic state at each carbon site of the complex. As a possible origin of the temperature variation of the electronic structure of the complex, the dynamic nature of the cyclopentadienyl ring and phenyl group was precisely investigated by the measurements of the spin−lattice relaxation rate of proton NMR and by the incoherent neutron scattering.

Experimental Section

$ZrCp_2$(DPBD) was synthesized as shown in Figure 1. This method is similar to the previously reported one.[10] The complex is air- and moisture-sensitive. Sample preparation for all measurements was conducted in a glove box filled with dry N_2 gas or dry He gas.

^{13}C-CP/MAS NMR spectra were measured at the resonance frequency of 75.47 MHz with Bruker DSX300 spectrometer with a conventional zirconium rotor (7 mm). The sample was packed to the rotor in the glovebox and the rotor was quickly transferred to the CP/MAS NMR probe through the Bruker

* Corresponding author. E-mail: takeda@chem.sci.osaka-u.ac.jp. Fax: (+81) 6-843-7744.
† Department of Chemistry, Faculty of Science.
‡ Department of Macromolecular Science, Faculty of Science.
§ Department of Chemistry, Faculty of Engineering Science.
⊗ Abstract published in *Advance ACS Abstracts,* December 15, 1996.

S1089-5647(96)01978-5 CCC: $14.00

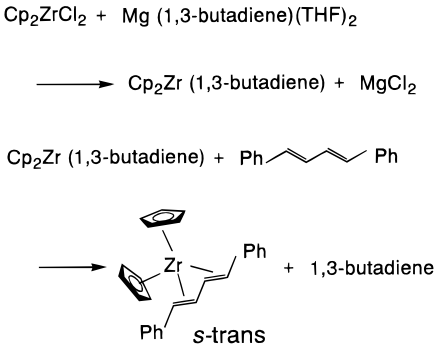

Figure 1. Scheme of the synthesis of $ZrCp_2$(DPBD).

sample guide tube. Dry N_2 gas evaporated from the liquid N_2 container was used as bearing and driving gas for magic angle spinning. This procedure keeps the sample in oxygen- and moisture-free condition. Decomposition of the sample was not detected during the measurements. ^{13}C-CP/MAS NMR spectrum of the decomposed material, the color of which is light yellow, was also measured. The spectrum of the decomposed material is completely different from that of $ZrCp_2$(DPDB). The contact time was 1 ms and the $\pi/2$ pulse length was 5 μs for both ^{13}C and ^{1}H nuclei. The number of accumulations was between 200 and 900, and repetition time was between 10 and 50 s depending on the spin−lattice relaxation time of the proton. The chemical shift was measured from TMS, and hexamethylbenzene was used as an external reference. The thermometer of the CP/MAS NMR probe was calibrated by the contact shift of carboxyl carbon of $Sm(CH_3COO)_3{\cdot}4H_2O$[11] under the same spinning condition for $ZrCp_2$(DPDB). The uncertainty of the temperature was 5 K.

The spin−lattice relaxation rate, T_1^{-1}, of proton was measured at 18.0 and 37.2 MHz. The $\pi/2$ train−τ−$\pi/2$ pulse sequence was employed. The magnetization recovery curve was expressed by a single-exponential function. The temperature was kept constant within ±0.2 K and was measured by chromel−p-constantan and Au(Fe)−chromel thermocouples.

Neutron scattering spectrum was measured for 0.87 g of $ZrCp_2$(DPDB) with LAM-D spectrometer at the KENS pulsed neutron facility at National Laboratory for High Energy Physics, Japan.[12] Pyrolytic graphite ((002) reflection) was used as crystal analyzers which were located at scattering angles of ±35 and ±80° with respect to the incident neutron; the momentum transfer values are 0.9 and 1.9 Å^{-1} at the elastic peak position, respectively. The resolution of this spectrometer is 0.3 meV. The background signal was low and flat in the energy transfer region of interest. The observed spectrum was normalized to the incident neutron spectrum and the scattering function, $S(Q,\omega)$, was obtained after correction for the detector efficiencies by using vanadium reference sample. The temperature of the sample was controlled to ±0.2 K of the set point in a variable temperature refrigerator cryostat, for which a top loading system is installed.[13]

Results and Discussion

a. Thermochromism and ^{13}C-CP/MAS NMR Spectra. Thermochromism of $ZrCp_2$(DPBD) was observed visually for the polycrystalline sample sealed in a glass ample with He gas for heat exchange. The deep purple color at room temperature changes continuously to light red as the temperature is decreased down to 77 K. The thermochromism is not due to a structural phase transition of the crystal, since no heat anomaly was detected by the differential thermal analysis between 100 and 300 K. We tried to measure the absorption spectrum in the visible and ultraviolet regions (between 10 000 and 30 000 cm^{-1}) for the powdered sample dispersed in KBr disk between 9 and 300 K. Two broad absorption maxima were observed near 19 000 and 23 000 cm^{-1}, and an increase of the optical density together with broadening and significant red shift of the two peaks were observed as the temperature was increased. However, for the quantitative discussion of the optical property of the complex, a reflection experiment on the single crystal is required and has not yet been successful due to the difficulty of preparing the single crystal with good surface. The two absorption peaks were assigned to the HOMO−LUMO and HOMO−LUMO+1 transitions with the aid of semiempirical molecular orbital calculations (Zener's INDO/1-ZINDO).[14] The calculated absorption bands locate at 19 300 (HOMO−LUMO) and 21 000 cm^{-1} (HOMO−LUMO+1). The HOMO, LUMO, and LUMO+1 are mainly composed of the d-orbitals of Zr and the π-orbitals of DPBD molecule and Cp rings. The discussion of the MO calculation is summarized in the subsection c.

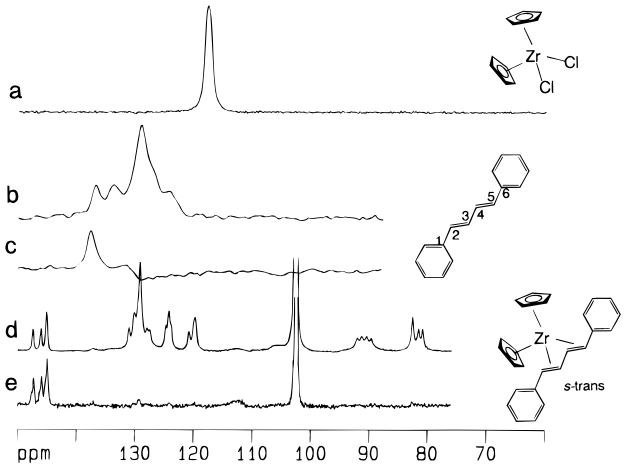

Figure 2. ^{13}C-CP/MAS NMR spectra for polycrystalline samples at room temperature: (a) $ZrCp_2Cl_2$, (b) 1,4-diphenyl-1,3-butadiene (DPBD), (c) dipolar dephasing CP/MAS NMR spectrum of DPBD, (d) $ZrCp_2$(DPBD), and (e) dipolar dephasing CP/MAS NMR spectrum of $ZrCp_2$(DPBD).

The thermochromism of $ZrCp_2$(DPBD) indicates the temperature variation of the electronic state of the complex, which may be detected by the chemical shift of ^{13}C-CP/MAS NMR spectrum of DPBD molecule and cyclopentadienyl rings of the complex. Before we discuss the temperature variation of the ^{13}C chemical shift, the ^{13}C-CP/MAS NMR spectrum of the complex is compared with the spectra of precursors, DPBD and $ZrCp_2Cl_2$. The chemical shift of the cyclopentadienyl ring (Cp ring) which is 117.8 ppm for $ZrCp_2Cl_2$ is largely shifted to high field (102.6 ppm) by constructing the complex, $ZrCp_2$(DPBD), as shown in Figure 2, a and d. In spite of the fact that the direct bonding between Cp ring and Cl or DPBD does not exist, the chemical shift shielding becomes remarkably large for $ZrCp_2$(DPBD). The indirect interaction between Cp ring and DPBD through the d-electron of Zr is significant. The peaks except 102.6 ppm in the spectrum d come from the DPBD molecule. The chemical shifts of the ^{13}C of DPBD in the complex are largely shifted by mixing of d-electron of Zr (spectrum d), while all carbon signals of the DPBD molecule in its crystalline state appear in the typical shift region for the aromatic carbons (spectrum b). The result indicates that the electronic structure of the organic π-conjugated system is largely changed. To investigate how much change of the chemical shift occurs at each carbon site, the signals were assigned. The NMR signals of the carbons (1 and 6) of the phenyl rings, which are not directly bonded to proton, are selectively observed by

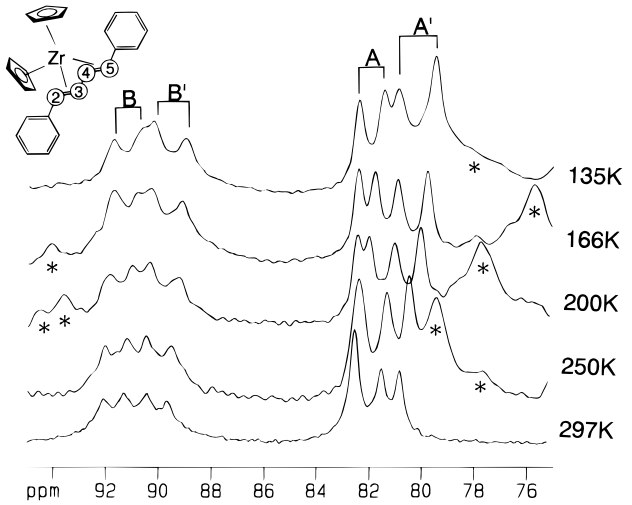

Figure 3. Temperature variation of the ^{13}C-CP/MAS NMR spectrum of the butadiene framework. Two pairs of peaks, A and A′, are the signal of carbons 3 and 4, while B and B′ are carbons 2 and 4. Asterisks designate the spinning side bands.

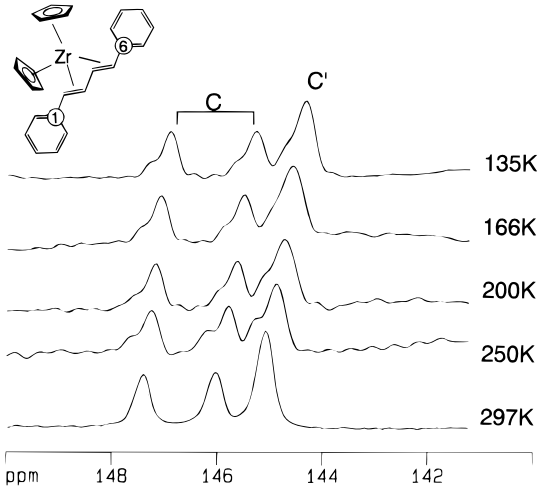

Figure 4. Temperature variation of the ^{13}C-CP/MAS NMR spectrum of carbons 1 and 6 of the phenyl groups.

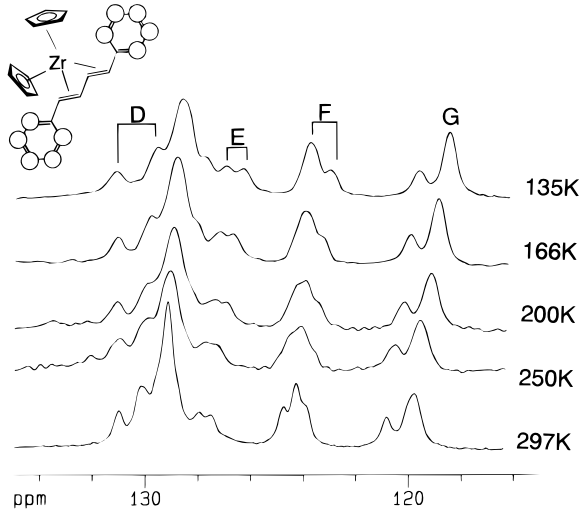

Figure 5. Temperature variation of the ^{13}C-CP/MAS NMR spectrum of the carbons of the phenyl groups except 1 and 6.

employing the dipolar dephasing technique of CP/MAS NMR.[15] The chemical shifts (137.6 ppm in spectrum c) of DPBD is shifted to low field (147.4, 146.0, and 145.1 ppm in spectrum e) for $ZrCp_2$(DPBD). The splitting of the signal in spectrum e is due to the lack of symmetry of the complex in the crystal and two crystallographically nonequivalent complexes in the unit cell.[4] Thus four different signals may be observed at maximum and two of the four signals coincide with each other in the spectrum e. The assignment of other carbon signals in the spectrum d is based on the combination of heteronuclear indirect spin coupling between ^{1}H and ^{13}C in ^{13}C NMR, homonuclear one in ^{1}H NMR, and ^{1}H−^{13}C HETCOR NMR in deuterated benzene solution. The largely shifted peaks which appeared at 82.6, 81.6, and 80.9 ppm were assigned to the carbons 3 and 4 (80.4 ppm in solution) and peaks at 92.1, 91.3, 90.5, and 89.7 ppm to the carbons 2 and 5 (88.3 ppm in solution). Here we note that ambiguous assignment of ^{1}H NMR signals reported previously is corrected.[10] The splittings of carbon signals are also due to the crystallographically nonequivalent sites of the carbons. Consequently, the ^{13}C-CP/MAS NMR spectra indicate that the remarkable change of the electronic state by addition of Zr propagates all over the DPBD molecule in the complex. Particularly, it is noted that the chemical shifts of several carbons of the phenyl rings are remarkably changed by constructing the complex, indicating that the π-conjugation including the phenyl rings is changed. This observation is closely related to the origin of the deep color of the complex. The thermochromism is connected to the temperature variation of the electronic state at each carbon site in the complex, which was detected by variable-temperature ^{13}C-CP/MAS NMR spectrum.

Figure 3 shows the temperature dependence of the ^{13}C chemical shift of the butadiene framework. The three peaks between 80.9 and 82.6 ppm at 297 K are the signals of carbons 3 and 4. The peak at 82.6 ppm at 297 K splits in two peaks and the separation between the two peaks, 80.9 and 81.6 ppm, becomes larger as temperature is decreased. This result indicates that two pairs of peaks, A and A′, shown in Figure 3, come from two crystallographically independent complexes in a unit cell[4] and the magnitude of the nonequivalence between the two carbons, 3 and 4, of DPBD becomes large as temperature is decreased. Very similar behavior was observed for two pairs of peaks, B and B′ in Figure 3, which were assigned to the carbons 2 and 5. The chemical shifts of the phenyl carbons are also temperature dependent as shown in Figures 4 and 5; the splittings in the pairs C, D, E, and F become large and the peaks C′ and G are shifted as temperature is decreased. The peak of the Cp ring is not split but is shifted to high field as shown in Figure 6. The temperature variations of the ^{13}C chemical shifts, especially the splitting, indicate that the distortion of the electronic structure of the complex becomes continuously large as temperature is decreased and is expected to become much larger below 135 K. This temperature variation of the chemical shifts and thus of the electronic state at each carbon site of the complex is closely related to the thermochromism. Here, it is interesting to know what is the origin of the temperature variation of the electronic structure at each carbon site. A possible mechanism is the motions of the molecular groups of the complex in the solid state.

b. Dynamics of Cp Ring and Phenyl Ring in the Solid State. *1. Spin−Lattice Relaxation Rate of Proton NMR.* To investigate the dynamic behavior of the complex in the solid state, the spin−lattice relaxation rate T_1^{-1} of proton NMR was measured between 14 and 300 K at 18.0 and 37.2 MHz. The result of the measurement is shown in Figure 7. Two maxima were clearly observed near 50 K ($10^3(1/T) = 20$ (1/K)) and 100 K ($10^3(1/T) = 10$ (1/K)), indicating that the two motional modes are thermally excited. The high-temperature mode with the activation energy of 84 ± 5 meV[16] was assigned to the 180° flip motion of the phenyl ring around the C−C bond and the

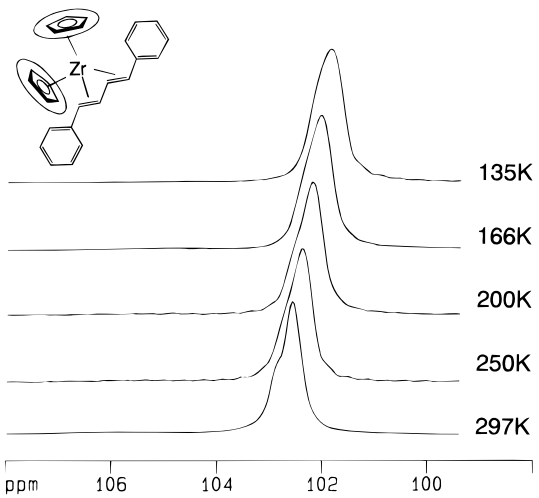

Figure 6. Temperature variation of the ^{13}C-CP/MAS NMR spectrum of the Cp rings.

low-temperature mode with the small activation energy of 28 ± 1 meV was assigned to the rotation of the Cp ring about the fivefold axis. The break of the slope of T_1^{-1} below 20 K ($10^3(1/T) \geq 50$ (1/K)) was attributed to the excitation energy 5.0 ± 0.5 meV between the torsional ground state and the first excited state of the Cp ring as discussed below.

The T_1^{-1} was calculated by assuming the two motional modes mentioned above. For the rotation of the Cp ring around its fivefold axis, the relaxation formula due to the fluctuation of the nuclear dipole interaction between protons in a Cp ring was derived according to the master equation of the spin−lattice relaxation[17−19] without cross-correlation effect[20] and is expressed by

$$T_1^{-1}(\text{intra Cp}) = A_{dd}(\text{intra Cp})\left(\frac{\tau_1}{1+\omega_0^2\tau_1^2} + \frac{4\tau_1}{1+4\omega_0^2\tau_1^2} + \frac{\tau_2}{1+\omega_0^2\tau_2^2} + \frac{4\tau_2}{1+4\omega_0^2\tau_2^2}\right) \quad (1)$$

where

$$A_{dd}(\text{intra Cp}) = m \times \frac{9}{4}\gamma^4\hbar^2 \times \frac{8}{75}\left(3\cos^2\frac{3\pi}{5} - 1\right)\left(\cos\frac{2\pi}{5} + \cos\frac{4\pi}{5}\right)/R^6 \quad (2)$$

and

$$\tau_1^{-1} = 2\left(1 - \cos\frac{2\pi}{5}\right)\Gamma = 1.38\Gamma \quad (3)$$

$$\tau_2^{-1} = 2\left(1 - \cos\frac{4\pi}{5}\right)\Gamma = 3.62\Gamma$$

Γ is jumping rate between the two neighboring wells of fivefold potential and can be expressed by Arrhenius relation, $\Gamma = \Gamma_0 \exp(-E_a/kT)$, for the classical limit. The quantity m (=10/24) is the fraction of protons of Cp rings among all protons included in the complex. R is the distance between the neighboring protons in the regular Cp ring and $R = 2.71$ Å was used. The value of T_1^{-1}(intra Cp) was calculated (A_{dd}(intra Cp) = 1×10^8 s^{-2}) and is found to be smaller than the contribution from the dipole interaction between the protons of butadiene

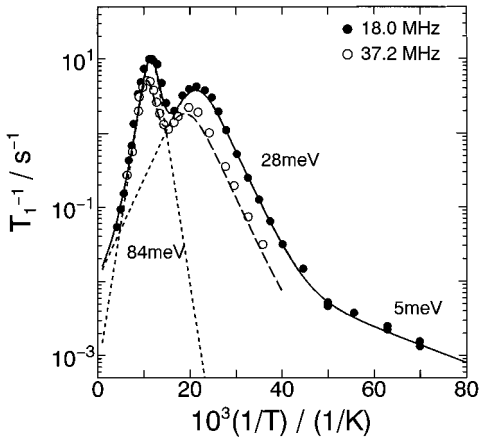

Figure 7. Temperature and frequency dependence of the spin−lattice relaxation rate of proton NMR. Open and closed circles are the observed values. Solid and broken curves are the sum of calculations for the Cp ring rotation and 180° flip rotation of the phenyl group. Dotted curves show the two components of T_1^{-1} at 18.0 MHz, *i.e.* Cp ring rotation (maximum at low temperature) and 180° flip rotation of the phenyl group (maximum at high temperature).

framework and Cp ring, *i.e.* T_1^{-1}(inter Cp), which can be expressed by

$$T_1^{-1}(\text{inter Cp}) = A_{dd}(\text{inter Cp})\left(\frac{\tau_0}{1+\omega_0^2\tau_0^2} + \frac{4\tau_0}{1+4\omega_0^2\tau_0^2}\right) \quad (4)$$

Since T_1^{-1}(inter Cp) is larger than T_1^{-1}(intra Cp) in the present case, the formula which is the same as eq 4 with A_{dd}(total Cp) instead of A_{dd}(inter Cp) was used as a good approximation for the analysis of the observed T_1^{-1} below 70 K ($10^3(1/T) \geq 15$ (1/K)). The solid and broken curves are the calculations for the different Larmor frequencies. Here A_{dd}(total Cp) = 3.0×10^8 s^{-2} was used and the following temperature dependence of the correlation time of the rotation of the Cp rings was derived,

$$\tau_0^{-1}(\text{Cp}) = 1.4 \times 10^{11} \exp(-28\ meV/kT) + 7.0 \times 10^5 \exp(-5\ meV/kT) \quad (5)$$

which is shown in Figure 8. The activation energy for the rotation of the Cp ring around its fivefold axis is 28 ± 1 meV, and the small activation energy 5.0 ± 0.5 meV in the low-temperature region was attributed to the excitation energy between the torsional ground and the first excited states. Here the quantum mechanical tunneling of the Cp ring through the torsional first excited state seems to dominate T_1^{-1}. This phenomenon is similar to the tunneling of methyl groups, which has been well investigated experimentally and theoretically.[21−26] In this case, the Larmor frequency dependence of the spin−lattice relaxation rate is useful to estimate the tunneling frequency[26] and was measured for $ZrCp_2$(DPBD) between 3 and 40 MHz at 17.9 K by use of the field cycling technique.[27] The observed frequency dependence almost obeys the relation $T_1^{-1} \propto \omega_0^{-2}$ at the high-frequency region and tends to a smaller slope below ca. 10 MHz. This trend is not the case of the relaxation due to paramagnetic impurities ($T_1^{-1} \propto \omega_0^{-0.5}$ for the wide-frequency region) but is very similar to the rotational tunneling of methyl group with the tunneling frequency of the order of Larmor frequency.[26] The torsional excitation energy was estimated by the calculation of the energy scheme for the Cp ring rotation with the moment of inertia $I = 1.9 \times 10^{-45}$ kg m^2 around the fivefold axis. The energy levels were calculated by numerical diagonalization of the energy matrix, where a series

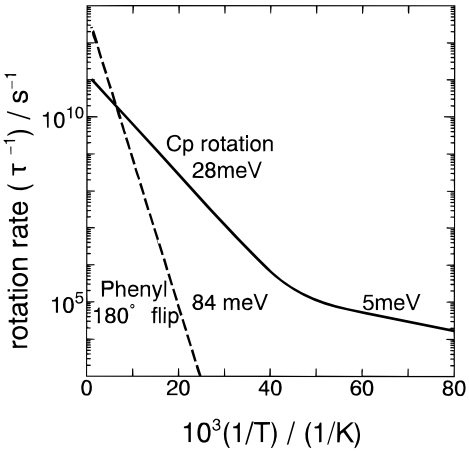

Figure 8. Temperature dependence of the rate of Cp ring rotation (solid curve) and that of the 180° flip rotation of the phenyl group (broken line).

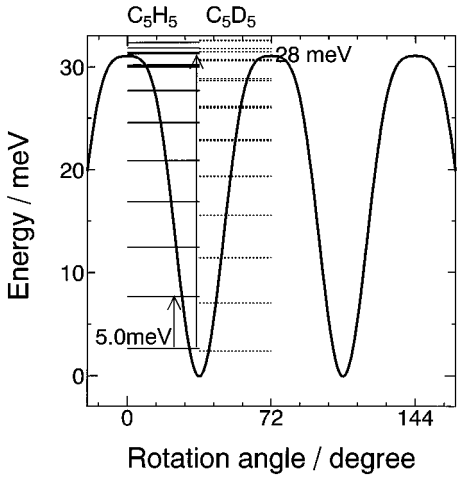

Figure 9. Potential function and torsional energy scheme of Cp ring and its deuterated derivative.

expansion into the free rotor state for the wave function was used.[28] The convergence of the energy levels was examined by enlarging the matrix size up to 90 × 90. Assuming the pure fivefold potential compatible with the observed activation energy (28 meV), the torsional excitation energy was calculated to be 3.6 meV. The value is smaller than the experimental one (5 meV), and the calculation was improved by adding higher order terms as usually assumed.[24,29] The parameters of the potential were chosen so that the activation energy (28 meV) and the torsional excitation energy (5 meV) determined above agree with the calculation. These criteria do not uniquely fix the parameter values and therefore we adopted the potential function as simple as possible. As a result of trial and error calculations, we obtained two reasonable potential functions with a higher order of 10-fold term. One is

$$V/\text{meV} = 15.6\{1 + \cos(5\theta)\} - 3.7\{1 + \cos(10\theta)\} + 7.3 \quad (6)$$

and is shown in Figure 9. The torsional levels for the deuterated Cp ring ($I = 2.3 \times 10^{-45}$ kg m^2) are also shown by dotted lines. The torsional ground state has 5-fold degeneracy. The other potential function is

$$V/\text{meV} = 10.3\{1 + \cos(5\theta)\} + 9.8\{1 + \cos(10\theta)\} - 9.0 \quad (7)$$

which has small subminima in the bottom of the potential curve due to the large contribution of the 10-fold potential term. In this case the degeneracy of the torsional ground state is 10-fold. In both cases of eqs 6 and 7, torsional ground state exhibits small tunneling splittings of the order of a few megahertz or less. This is almost consistent with the observed Larmor frequency dependence of T_1^{-1}. Discussions of the hindering potential for the rotation of Cp ring have been reported for metallocene compounds,[29−33] particularly for the low-temperature phase of $NiCp_2$ the structure of the potential function has been discussed precisely from the unusual temperature dependence of the torsional excitation band of the Cp ring.[29] The torsional excitation energy of 4.6 meV for $NiCp_2$[29] is similar to 5 meV for $ZrCp_2$(DPBD), whereas the activation energy of 65 meV for $NiCp_2$[32] is larger than 28 meV for $ZrCp_2$(DPBD). This is not surprising, since the shape of the potential function is sensitive to the packing arrangement of molecules in the crystal. It was reported for $FeCp_2$ that the activation energy and the torsional excitation energy are largely changed by undergoing the structural phase transition.[30,31]

The observed activation energy for the rotation of the Cp ring in the complex $ZrCp_2$(DPBD) is very small among the zirconocene complexes investigated hitherto.[34,35] This is an unique character of this complex. Since the activation energy 28 meV corresponds to the thermal energy at 310 K, the thermal population of the Cp ring near the top of the barrier is large for this complex near room temperature and the fluctuation amplitude of the Cp ring is extremely large. This fact is in good agreement with the very large thermal ellipsoid of the Cp ring observed by the X-ray diffraction experiment.[4] This motion perturbs the bonding between the Cp ring and zirconium.

For the dynamical perturbation on the electronic state of the π-conjugated system of the complex, the motion of the phenyl ring seems also important. It was revealed that the phenyl rings undergo 180° flip rotation with the activation energy of 84 ± 5 meV. This motion was observed as a high-temperature maximum of T_1^{-1} of proton NMR as shown in Figure 7. The relaxation formula due to the flip motion of the phenyl ring is the same as that of eq 4. The magnitude of the fluctuation of the dipole interaction A_{dd}(Ph(180°)) was estimated by using the conformation of DPBD. The calculated value within a complex is 7×10^8 s^{-2} which is consistent with 8×10^8 s^{-2} deduced from the maximum value of the T_1^{-1} near 100 K (10^3 (1/T) = 10 (1/K)). The rate of the 180° flip motion of the phenyl ring around the C−C bond is expressed by the Arrhenius formula

$$\tau_0^{-1}(\text{Ph}(180°)) = 6.7 \times 10^{12} \exp(-84\ \text{meV}/kT) \quad (8)$$

which is slow in the low-temperature region and is the same order near the room temperature compared with the rate of the Cp ring rotation as shown in Figure 8. The rotational motion of the phenyl ring induces a fluctuation of the π-conjugation of the DPBD molecule in the complex $ZrCp_2$(DPBD).

2. Incoherent Neutron Scattering. To investigate the torsional modes of the Cp ring and the phenyl ring, incoherent neutron scattering spectrum was measured in the energy transfer region between −3 and 200 meV. In this report the energy transfer region below 20 meV is discussed in which the torsional modes of the Cp ring and of the phenyl ring are expected to be observed. Figure 10 shows the neutron scattering spectrum measured at 15, 60, and 150 K. Four spectra with two different momentum transfer values (0.9 and 1.9 Å^{-1}) accumulated simultaneously were added to improve the statistics for each temperature. A characteristic feature of the spectrum observed at 15 K is a broad unresolved peak below 10 meV, in which several excitations overlap. In addition to the torsional excita-

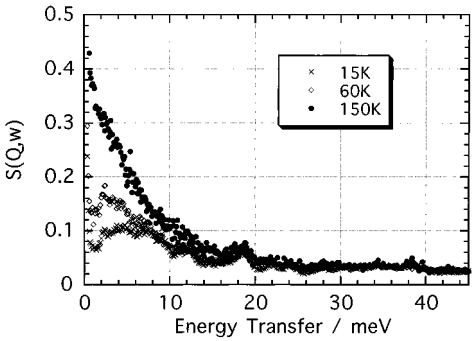

Figure 10. Incoherent neutron scattering spectrum of $ZrCp_2$(DPBD) measured at 15 K (×), 60 K (◇), and 150 K (●).

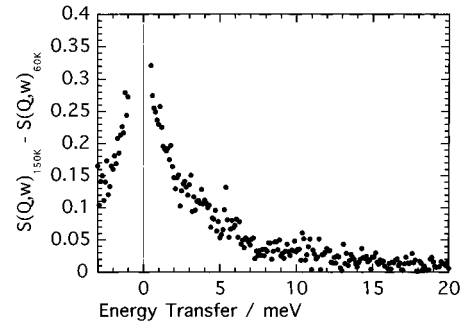

Figure 11. Quasielastic neutron scattering from $ZrCp_2$(DPBD) at 150 K. The quasielastic component was separated by subtracting the scattering function $S(Q,\omega)_{60\ K}$ at 60 K from that at 150 K.

tion of Cp ring around 5 meV and its overtone, the torsional mode of the phenyl ring around the C−C bond and its overtones are expected to appear in this energy transfer region. A crude estimate of the fundamental excitation of the torsional oscillation of the phenyl ring is ∼3 meV. The cyclic twofold potential function, V/meV = 42.1(1 + cos(2θ)), which is consistent with the observed activation energy of 84 meV for the 180° flip motion of the phenyl ring, was assumed and the moment of inertia, $I = 1.37 \times 10^{-45}$ kg m^2, was used. Overlapping of these torsional modes of the Cp ring and the phenyl ring gives the broad unresolved scattering peak.

At elevated temperature, *i.e.* 150 K, the scattering intensity around the elastic peak is remarkable (Figure 10), although the intensity is much smaller than the elastic one. The result indicates that a rapid motion associated with the fluctuation of protons occurs at 150 K, while this motion is slow and cannot be detected by the neutron scattering at 60 K. The quasielastic scattering component at 150 K was separated from the elastic and inelastic scattering by subtracting the scattering function $S(Q,\omega)$ at 60 K from that at 150 K and is shown in Figure 11. The half-width at half-maximum (hwhm) of the observed quasielastic scattering is about 2 meV. Hwhm for the fivefold rotation of the Cp ring was calculated with the usual method[36] by taking into account the jumping rate 1.8×10^{10} s^{-1} at 150 K deduced from the proton NMR relaxation measurement. The hwhm is 17 and 24 μeV for the different momentum transfer values, 0.9 and 1.9 Å^{-1}, respectively. The hwhm for the 180° flip motion of the phenyl ring was also calculated to be 0.12 meV from the jumping rate 1.5×10^{10} s^{-1} determined by the proton NMR. These values are much smaller than the observed one (2 meV) and the rapid fluctuation detected as the quasielastic scattering is the third motional mode. It is noteworthy that the fluctuation amplitude of the third motional mode is so small as to be not detected by T_1^{-1} of proton NMR. The dependence of the quasielastic scattering of neutrons on the momentum transfer value is useful to estimate the geometry of the motion. Although the scattering intensity at $Q = 1.9$ Å^{-1} is larger by about 1.5 times than that at $Q = 0.9$ Å^{-1} and hwhm is the same for the two momentum transfer values within error, it was difficult to determine unambiguously the geometry of the rapid fluctuation because of the limited momentum transfer values obtainable with the instrument employed. The rapid fluctuation will give rise to a significant thermal parameter for the structure determination. Such large values of the equivalent isotropic thermal parameters were found for the phenyl carbons except for one linked to the butadiene framework by the X-ray diffraction experiment at room temperature in addition to the larger ones for the Cp ring.[4]

c. Electronic Structure Calculation. Semiempirical molecular orbital calculations were carried out using the INDO/1 electronic structure formalism developed by Zerner (ZINDO, Zerner's intermediate neglect of differential overlap program).[14] This method is known to be useful for the semiquantitative discussion of the optical property of the organometallic compounds.[37] The geometry of the complex determined by X-ray diffraction experiment was used for the calculations. To estimate the absorption spectrum, 14 orbitals around HOMO and LUMO were used for the configuration interaction. The two observed absorption bands in the visible region, which are responsible for the thermochromism, were assigned to the HOMO−LUMO and HOMO−LUMO+1 transitions. The calculated absorption bands locate at 19 300 and 21 000 cm^{-1} in reasonable agreement with the observed ones, 19 000 and 23 000 cm^{-1}. The lower frequency band 19 300 cm^{-1} is almost characterized by HOMO−LUMO transition, while the higher frequency one is determined by HOMO−LUMO+1 transition. All other calculated transitions exist in the ultraviolet region (higher than 27 000 cm^{-1}). The HOMO, LUMO, and LUMO+1 are mainly composed of the d-orbitals of Zr and the π-orbitals of butadiene framework. It is also noted that the π-orbitals of the Cp rings and the phenyl rings contribute to these orbitals. Therefore, these molecular orbitals can be modified by the rotation of the Cp ring and the phenyl ring. Indeed the calculated transition 19 300 cm^{-1} (HOMO−LUMO) shifted by an amount of 240 cm^{-1} with π/10 rotation of the Cp ring around the fivefold axis from the equilibrium position, where other parts of the complex were fixed in the original geometry. Although this calculation is qualitative, it is suggested that the thermochromism observed for $ZrCp_2$(DPBD) is caused by the thermal fluctuations of the Cp ring and the phenyl ring.

Concluding Remark

Thermochromism was observed for the organometallic complex $ZrCp_2$(DPBD) in the solid state. The change of the electronic state at each carbon site in the complex, which is closely related to the thermochromism, was detected by the variable-temperature ^{13}C-CP/MAS NMR. It was also revealed that the distortion of the electronic structure of the complex is large at low temperature in the solid state and is partially released as temperature is increased. The release of the distortion is mediated by the thermal excitation of the motional processes, *i.e.*, fivefold rotation of the Cp ring and 180° flip motion of the phenyl ring. The semiempirical calculation suggested that these motional modes modulates the HOMO, LUMO, and LUMO+1, which are responsible for the thermochromism. The motional modes were characterized by the measurements of the spin−lattice relaxation rate of proton NMR.

This study demonstrated that the electronic state of the organometallic complex with a large π-conjugated system is highly sensitive to the thermal fluctuation of the molecular groups of the complex. The complex ZrCp2(DPBD) is a model

compound of the transition state structure of the zirconocene catalyst and the dynamic effect on the electronic state of the complex is also expected for the catalytic process of the zirconocene compounds in solution.

Acknowledgment. The authors are grateful to Prof. K. Yakushi of Institute for Molecular Science for his support for the preliminary measurement of the optical property of the complex and also to Prof. S. Ikeda of National Laboratory for High Energy Physics and Dr. K. Shibata of Tohoku University for their help for the INS experiment. This research was supported by grant-in-aid to S.T., K.M., K.Y., and A.N. from the Ministry of Education, Science and Culture of Japan (Specially Promoted Research No. 06101004).

References and Notes

(1) Chien, J. C. W. *Polyacetylene: Chemistry, Physics, and Material Science*; Academic Press, Orland, 1984.

(2) Nakamura, A. *Bull. Chem. Soc. Jpn.* **1995**, *68*, 1515.

(3) Douglas, B. E.; McDaniel, D. H.; Alexander, J. J. *Concepts and Models of Inorganic Chemistry*; John Wiley & Sons, Inc.: New York, 1994; p 622.

(4) (a) Kai, Y.; Kanehisa, N.; Miki, K.; Kasai, N.; Mashima, K.; Nagasuna, K.; Yasuda, H.; Nakamura, A. *J. Chem. Soc., Chem. Commun.* **1982**, 191. (b) Kanehisa, N. Ph.D Thesis, Osaka University, 1992.

(5) Yasuda, H.; Tatsumi, K.; Nakamura, A. *Acc. Chem. Res.* **1985**, *18*, 120.

(6) Yasuda, H.; Nakamura, A. *Angew. Chem., Int. Ed. Engl.* **1987**, *26*, 723.

(7) Erker, G.; Krüger, C.; Müller, G. *Adv. Organomet. Chem.* **1985**, *24*, 1.

(8) Christensen, N. J.; Hunter, A. D.; Legzdins, P. *Organometallics* **1989**, *8*, 930.

(9) Okamoto, T.; Yasuda, H.; Nakamura, A.; Kai, Y.; Kanehisa, N.; Kasai, N. *J. Am. Chem. Soc.* **1988**, *110*, 5008.

(10) Yasuda, H.; Kajihara, Y.; Mashima, K.; Nagasuna, K.; Lee, K.; Nakamura, A. *Organometallics* **1982**, *1*, 388. Assignment of ^{1}H NMR signals reported in Table V of this reference is corrected. J-resolved ^{1}H signals around 3.17 ppm is assigned to protons bonded to carbons 3 and 4 (see text and Figure 2) and those around 3.83 ppm to protons bonded to carbons 2 and 5.

(11) Campbell, G. C.; Crosby, R. C.; Haw, J. F. *J. Magn. Reson.* **1986**, *69*, 191.

(12) Inoue, K.; Kanaya, T.; Kiyanagi, Y.; Shibata, K.; Kaji, K.; Ikeda, S.; Iwasa, H.; Izumi, Y. *Nucl. Instrum. Method Phys. Res.* **1993**, *A327*, 433.

(13) Takeda, S.; Shibata, K.; Ikeda, S. *KENS Report X*; Technical Information and Library, National Laboratory for High Energy Physics, Japan, 1995; p 206.

(14) (a) Pople, J. A.; Beveridge, D. L.; Dobosh, P. A. *J. Chem. Phys.* **1967**, *47*, 2026. (b) Ridley, J.; Zener, M. C. *Theor. Chim. Acta (Berlin)* **1973**, *32*, 111. (c) Ridley, J.; Zener, M. C. *Theor. Chim. Acta (Berlin)* **1976**, *42*, 223. (d) Bacon, A. D.; Zener, M. C. *Theor. Chim. Acta (Berlin)* **1979**, *42*, 21. (e) Zener, M. C.; Loew, G. H.; Kirchner, R. F.; Müller-Westerhoff, U. T. *J. Am. Chem. Soc.* **1980**, *102*, 589. (f) Anderson, W. P.; Cundari, T. R.; Drago, R. S.; Zener, M. C. *Inorg. Chem.* **1990**, *29*, 1. (g) ZINDO calculations were run on a CAChe system (CAChe Scientific, Inc., Sony/Tektronix Corp.).

(15) Opella, S.; Frey, M. H. *J. Am. Chem. Soc.* **1979**, *101*, 5854.

(16) 1 meV corresponds to 96.5 J/mol.

(17) Takeda, S.; Soda, G; Chihara, H. *Mol. Phys.* **1982**, *47*, 501.

(18) Imaoka, N.; Takeda, S.; Chihara, H. *Bull. Chem. Soc. Jpn.* **1988**, *61*, 1865.

(19) Onsager, L.; Runnels, L. K. *J. Chem. Phys.* **1969**, *50*, 1089.

(20) Lankhost, D.; Emid, S. *Physica* **1982**, *113B*, 57.

(21) Haupt, J.; Müller-Warmuth, W. *Z. Naturforsch.* **1968**, *23a*, 208.

(22) Haupt, J.; Müller-Warmuth, W. *Z. Naturforsch.* **1969**, *24a*, 1066.

(23) Haupt, J. *Z. Naturforsch.* **1971**, *26a*, 1578.

(24) Müller-Warmuth, W.; Schüller, R.; Prager, M.; Kollmar, A. *J. Chem. Phys.* **1978**, *69*, 2382.

(25) Takeda, S.; Fujiwara, T.; Chihara, H. *J. Phys. Soc. Jpn.* **1989**, *58*, 1793.

(26) Takeda, S.; Chihara, H. *J. Magn. Reson.* **1984**, *56*, 48.

(27) Takeda, S.; Chihara, H. *J. Magn. Reson.* **1983**, *54*, 285.

(28) (a) Clough, S.; Heideman, A.; Horsewill, A. H.; Paley, M. N. J. *Z. Phys. B* **1985**, *55*, 1. (b) Atake, T.; Gyoten, H.; Chihara, H.; *J. Chem. Phys.* **1982**, *76*, 5515. (c) Fujiwara, T. Ph.D Thesis, Osaka University, 1990.

(29) Chhor, K.; Lucazeau, G.; Souisseau, C. *J. Raman Spectrosc.* **1981**, *11*, 183.

(30) Campbell, A. J.; Fyfe, C. A.: Halord-Smith, D.; Jeffry, K. R. *Mol. Cryst. Liq. Cryst.* **1976**, *36*, 1.

(31) Gardner, A. B.; Howard, J.; Waddington, T. C. *Chem. Phys.* **1981**, *57*, 453.

(32) Sourisseau, C.; Lucazeau, G,: Dianoux, A. J.; Poinsignon, C. *Mol. Phys.* **1983**, *48*, 367.

(33) Raison, P.; Lander, G. H.; Delapalme, A.; Williams, J. H.; Kahn, R.; Carlile, C. J.; Kanellakopulos, B. *Mol. Phys.* **1994**, *81*, 369.

(34) Gilson, D. F. R.; Gomez, G.; Butler, I. S.; Fitzpatrick, P. J. *Can. J. Chem.* **1983**, *61*, 737.

(35) Braga, D. *Chem. Rev.* **1992**, *92*, 633.

(36) Bée, M.; *Quasielastic Neutron Scattering*; Adam Hilger: Bristol, U.K., 1988.

(37) Pfennig, B. W.; Thompson, M. E.; Bocarsly, A. B. *Organometallics* **1993**, *12*, 649.